A density functional approach of prototropic tautomerism of guanine

ARTICLE *in* CHEMICAL PHYSICS · FEBRUARY 2001

Impact Factor: 1.65 · DOI: 10.1016/S0301-0104(00)00359-1

2 AUTHORS, INCLUDING:

Shan Xi Tian
University of Science and Technology …

88 PUBLICATIONS **713** CITATIONS

SEE PROFILE

ELSEVIER

Chemical Physics 264 (2001) 187–196

Chemical Physics

www.elsevier.nl/locate/chemphys

A density functional approach of prototropic tautomerism of guanine

Shan Xi Tian *, Ke Zun Xu

Department of Modern Physics, University of Science and Technology of China, Hefei, P.O. Box 4, Anhui 230027, People's Republic of China

Received 13 June 2000

Abstract

Seven tautomeric species of guanine are studied through density functional calculations with various exchange-correlation functionals XαPL, XαLYP, and B3LYP, as well as the Hartree–Fock ab initio, using the 6-31G(d), 6-31+G(d,p) and D95V(d) basis sets. Corrections for the zero-point vibrational energy are included. Based on the self-consistent reaction field calculations with the Onsager or polarized continuum model approximation, it is found that guanine N(7)H[G5] is more stable than N(9)H[G1] tautomer in vacuum with 55 kcal mol^{-1} high energy barrier, which is inverse in water solution. We also investigate the thermodynamic effect on the distribution of the prototropic tautomers using transition state theory.

Keywords: Nucleic acid base; Guanine; Prototropic tautomerism; Transition states; Density functional method; Ab initio

1. Introduction

Nucleic acid bases govern the storage and transfer of genetic information, their geometrical and conformational properties have an important effect on their biochemical behavior. It is notable that there is a certain relationship between the occurrence of the rare tautomeric forms and spontaneous mutations developing during replication [1,2]. Theoretical predictions of the various physicochemical properties of the prototropic tautomers are of great importance in the studies of the reactivity of the nucleic acid bases and other heteroaromatic compounds. Many computational investigations have been aimed at accurately determining structures and properties of the nucleic acid bases and their tautomers [3–16].

Guanine is one of the most important nucleic acid bases occurring in both DNA and RNA, and as the largest nucleic acid base, it has the most complex tautomeric forms [16]. The infrared (IR) vibrational isolated matrix experiments presented more than three different tautomers [17–19]. Some papers have been devoted to studying guanine tautomerism, the tautomeric energies have also been investigated at ab initio and semiempirical levels [10,16,20–23]. Recently, Leszczynski performed an ab initio study with large basis sets and higher order electron correlation contributions on

* Corresponding author. Present address: Department of Chemistry, Graduate School of Science, Tohoku University, Aramaki, Aoba-ku, Sendai 980-8578, Japan. Tel.: +81-22-217-6576; fax: +81-22-217-6580.

E-mail address: sxtian@qpcrkk.chem.tohoku.ac.jp (S.X. Tian).

0301-0104/01/$ - see front matter
PII: S0301-0104(00)00359-1

the potential energy surface of guanine, in which four lowest energy tautomers were calculated at the MP4(SDTQ)/6-31G(d,p), MP4(SDQ)/6-311G-(d,p) and MP2/6-311++G(df,pd) levels [6,7]. Most of these studies only focused upon the oxy–hydroxy tautomeric process and presented some controversial stability orders. The present work is aimed to accurately determine the geometrical and electronic properties of guanine tautomers which are tautomerized from oxy–hydroxy or proton-shift of amino-group, the fully optimized geometries as well as the calculated values of dipole moments and dipole polarizability of the guanine tautomers are presented and compared with the previously theoretical and experimental results [10–12,16–26]. Transition state theory [27] is employed for studying thermodynamic and kinetic distribution of some tautomeric species in gas phase. Stability order of the tautomers is investigated both in gas phase and for solvent effects.

2. Theoretical methods

All density functional theory (DFT) computations as well as Hartree–Fock (HF) ab initio are performed with the GAUSSIAN 98W [28] program package. It has been proved extensively that the new developments of a variety of DFT methods, which are less expensive methods than MP2, have shown promising potential to predict geometries and vibrational spectra in good agreement with experimental results [29–31]. Especially, our previous work [15] also showed that the DFT-B3LYP functional, consisting of the Becke's three-parameter exchange functional (B3) [32,33] and the Lee–Yang–Parr (LYP) non-local correlation functional [34], succeeded in predicting the stability order and the geometrical parameters of the uracil tautomers in gas phase. So the method B3LYP is adopted here for optimizations without planarity constraints for the geometries of the minima and transition states of guanine, using the 6-31+G(d,p) and 6-31G(d) basis sets, respectively. The geometrical structures are diagnosed by the analyses of the harmonic vibrational frequencies. The 6-31G(d) and the Dunning–Huzinaga valence double zeta D95V(d) [35] basis sets are employed for single-point energy calculations by the DFT methods using various of exchange-correlation functionals XαPL, XαLYP, and B3LYP, as well as the HF ab initio. In the correlation-modified Xα methods, the XαPL and the XαLYP, the electron density $\rho^{4/3}$ with the empirical coefficient of 0.7 is used as the exchange functional (Xα) [36] which is modified by the combination with the local (non-gradient corrected) correlation functional of Perdew (PL) [37] or the LYP correlation functional. Corrections for zero-point vibrational energies (ZPVEs) and harmonic vibration frequencies are calculated at the B3LYP/6-31+G(d,p)//B3LYP/6-31G(d) level. The scaled factor of the present ZPVEs is 0.9804 [38]. Seven tautomeric species of guanine were investigated in this work, their molecular models are shown in Fig. 1. The transition states, which are between G1 and G2a, G1 and G3a, and G1 and G5, are located by the STQN method [39]. The solvent effects on the tautomeric equilibrium are considered by self-consistent reaction field (SCRF) calculations using the Onsager [40–43] and the polarized continuum models (PCM) developed by Tomasi et al. [44]. The cavity is spherical with a radius $a_0 = 3.767$ Å in the Onsager model [40–43]. The default values of the scaled van der Waals radii of the constituent atoms in the program GAUSSIAN 98W are used in the PCM calculations.

3. Results and discussions

3.1. Geometrical parameters

The geometrical parameters of the tautomers optimized at the B3LYP/6-31+G(d,p) level are given and compared with the MP2/6-31G(d,p) values of guanine [11], the geometrical parameters are tabulated in Table 1. We find that the heterocycles of G1, G2a, G2b, G3a, G3b, and G5, are approximately coplanar except for G4 with the most ~4° dihedral angle of the amino group from the plane. The changes in molecular geometries associated with the lactam–lactim tautomerism [G1–G2a(b)] are similar to our previous results [15]. The most significant of these changes are in the C6–O14 bond length (0.12 Å), the N1–C6

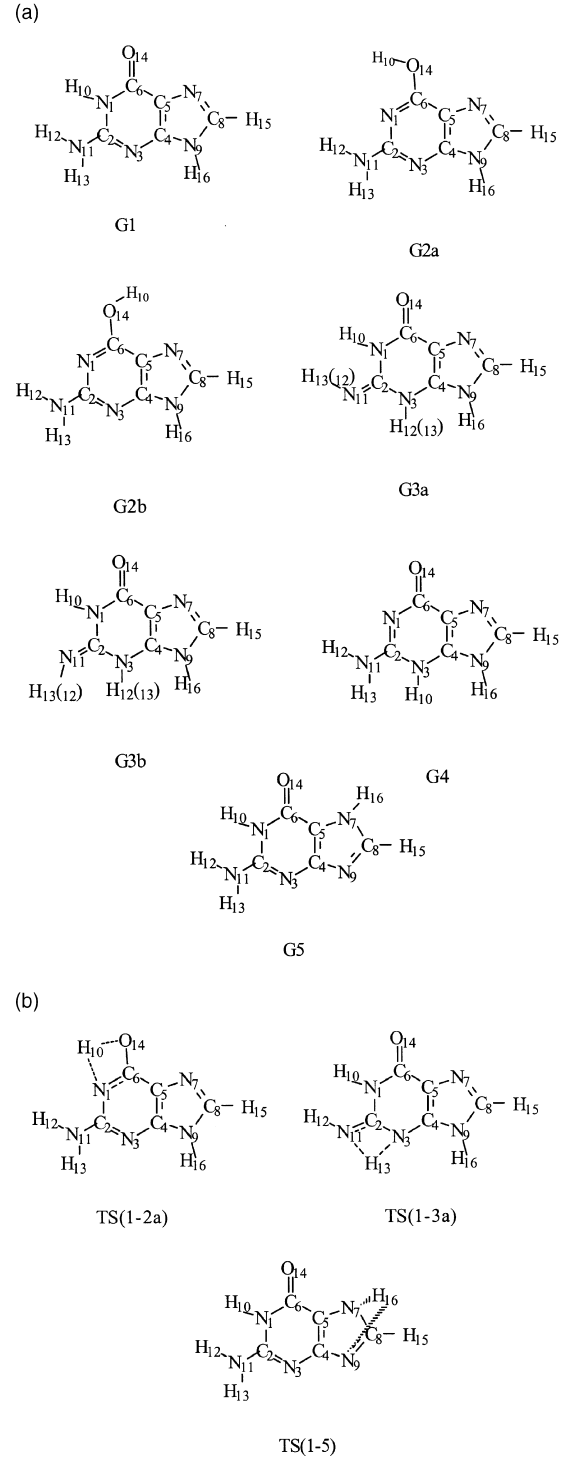

Fig. 1. (a) Seven tautomers and (b) some transition states of guanine.

bond length (0.11 Å), the internal angle at the carbonyl carbon (10°), and the corresponding asymmetric changes, 8° and 3°, in the two adjacent angles ∠C2N1C6 and ∠C4C5C6, respectively. There are no significant differences between the *cis*-lactim tautomer G2a and the *trans*-lactim tautomer G2b. The similar changes occur in the amine–imine tautomerism [G1–G3a(b)], but there are some differences between G3a and G3b, especially, for ∠C2N1H10 (2.4°) and ∠N1C2N11 (7.5°). The proton-shifts between N1 and N3, N7 and N9, occur in the different two heterocycles. It is found that there are different changes in G4 and G5 compared with the geometry of G1. The largest structural changes in G4 are in the angles ∠N3C4C5 (5.5°), ∠N1C6C5 (4.8°), and ∠C2N1C6 (3.8°), of the six-heterocycle. There are no significant differences of the bond lengths and the bond angles in the five-heterocycle of G4 compared with those of G1. It is interesting that the proton-shift from N9 to N7 in G5 brings about the changes in the angles ∠C4C5N7 (5.2°), ∠N9C4C5 (5.3°), ∠N3C4C5 (4.9°), and ∠C4C5C6 (4.1°). The proton-shift causes the significant changes of the amino structure. The geometrical parameters of G1 optimized in this work are very close to the previous MP2/6-31G(d,p) results [11]. The differences between the present and the MP2 values of the bond lengths are not over 0.02 Å or the angles are not over 1° except for the angles of the amino group. The different values of the angles in the amino groups may be caused by the diffuse functions added to the nitrogen and oxygen atoms in the basis 6-31+G(d,p) of the present work.

3.2. Molecular properties

Dipole moments of the seven tautomers calculated at the B3LYP/6-31G(d) level over the B3LYP/6-31+G(d,p) geometries are shown in Table 2. The values of the dipole moments are very different from each other's. The largest value of G4 is about five times higher than the smallest value of G5. When we compare the present values with the previous results [8,11,16,23] of the G1 dipole moment, it is found that the LDF result obtained with a double numerical basis set with 2p polarization functions on hydrogen atoms [8] is much larger,

Table 1
Geometrical parameters (bond length in Å, angles in deg.) of the guanine tautomers and their transition states obtained at the B3LYP/6-31+G(d,p) level

Parameters	G1	G2a	G2b	G3a	G3b	G4	G5	Ref. [11][a]
R(1,2)	1.372	1.357	1.358	1.395	1.390	1.292	1.383	1.371
R(2,3)	1.313	1.342	1.347	1.398	1.406	1.397	1.305	1.309
R(3,4)	1.359	1.335	1.333	1.366	1.374	1.379	1.367	1.364
R(4,5)	1.396	1.407	1.401	1.384	1.381	1.378	1.397	1.392
R(1,6)	1.438	1.329	1.322	1.425	1.416	1.420	1.418	1.428
R(6,5)	1.440	1.404	1.405	1.450	1.455	1.468	1.426	1.441
R(5,7)	1.382	1.388	1.387	1.383	1.382	1.385	1.379	1.375
R(7,8)	1.309	1.307	1.310	1.303	1.304	1.305	1.365	1.322
R(4,9)	1.370	1.374	1.377	1.365	1.366	1.367	1.373	1.368
R(9,8)	1.386	1.388	1.387	1.398	1.397	1.394	1.322	1.373
R(10,1)	1.014	–	–	1.013	1.013	–	1.014	1.011
R(11,2)	1.376	1.369	1.367	1.282	1.282	1.385	1.380	1.383
R(12,11)	1.010	1.008	1.008	1.018	–	1.013	1.011	1.009
R(13,11)	1.011	1.008	1.008	–	1.018	1.013	1.012	1.009
R(14,6)	1.221	1.341	1.346	1.219	1.219	1.220	1.230	1.224
R(14,10)	–	0.972	0.971	–	–	–	–	–
R(3,10)[b]	–	–	–	–	–	1.012	–	–
R(16,9)	1.010	1.009	1.010	1.010	1.010	1.010	–	1.007
R(7,16)	–	–	–	–	–	1.010	–	–
A(1,2,3)	123.4	126.9	127.6	113.8	113.9	125.3	124.2	124.0
A(2,3,4)	112.7	112.1	111.8	120.3	119.9	114.7	114.5	111.6
A(3,4,5)	129.1	127.4	126.7	125.0	124.9	123.6	124.2	129.5
A(1,6,5)	126.5	118.7	118.2	130.1	130.5	122.7	125.3	127.0
A(4,5,6)	118.6	114.3	115.3	119.5	119.6	119.6	122.7	118.9
A(1,6,5)	109.7	120.6	120.4	111.4	111.4	113.9	109.2	109.0
A(4,5,7)	110.9	111.1	111.6	110.2	110.2	109.6	105.7	111.6
A(5,7,8)	104.7	104.2	104.1	105.3	105.4	105.5	106.0	103.8
A(5,4,9)	105.0	104.6	104.3	106.3	106.4	107.1	110.3	104.7
A(7,8,9)	112.7	113.4	113.2	112.3	112.2	112.4	113.3	112.9
A(4,9,8)	106.7	106.7	106.9	106.0	105.9	105.4	104.7	107.0
A(2,1,10)	120.1	–	–	116.6	114.2	–	120.1	119.3
A(2,3,10)	–	–	–	–	–	118.7	–	–
A(1,2,11)	117.1	115.9	115.5	128.2	119.7	120.7	115.9	116.0
A(2,3,13)	–	–	–	115.4	–	–	–	–
A(2,3,12)	–	–	–	–	117.9	–	–	–
A(1,6,14)	119.1	118.3	117.3	119.6	120.3	120.9	121.2	120.0
A(4,9,16)	125.6	125.8	126.0	127.5	127.7	128.0	–	125.4
A(5,7,16)	–	–	–	–	–	126.2	–	–
A(2,11,12)	118.3	117.4	117.5	112.6	–	111.8	117.8	115.3
A(2,11,13)	113.7	117.2	117.8	–	112.8	116.9	112.6	111.0
A(12,11,13)	114.7	118.1	118.8	–	–	113.4	114.0	112.3
A(6,14,10)	–	106.9	108.5	–	–	–	–	–
D(12,11,2,1)	−31.4	−16.4	−4.3	0.02	–	−7.24	−35.9	−42.2
D(13,11,2,3)	12.0	15.5	14.4	–	−0.08	41.6	10.8	12.1

[a] The geometrical parameters of G1 optimized at the MP2/6-31G(d,p) level [11].
[b] The same values of bond length N3-H12(13) in G3a(b) and N3-H10 in G4.

while the MP2 value (using the larger [5s3p2d]/(3s2p) basis) [11] and the SCF/6-31G* value of Roberts et al. [23] are close to the present result which is the medium of the values of G1 obtained by Sabio et al. using the semiempirical AM1 and SCF/3-21G methods [16]. Until now, the experi-

Table 2
Dipole moments (in Debye) of the guanine tautomers predicted at the B3LYP/6-31G(d) level over the B3LYP/6-31+G(d,p) geometries

Tautomer	μ_x	μ_y	μ_z	μ	μ^a	μ^b	μ^c
G1	−3.36	−5.60	0.81	6.58	6.79	7.27	6.41
G2a	−1.30	−2.80	0.70	3.17	3.04		
G2b	1.35	−3.17	0.64	3.45			
G3a	0.90	−5.88	0.00	5.94			
G3b	1.89	−8.48	0.00	8.69			
G4	−1.02	−10.64	0.45	10.69	11.1		
G5	−1.45	0.98	0.89	1.96			

[a] The SCF ab initio/6-31G* results of Ref. [23].
[b] The LDF/DN+d value of Ref. [8].
[c] The extrapolated MP2 value of Ref. [11].

Table 3
Dipole polarizabilities and the components, anisotropies (in atomic unit) of the guanine tautomers obtained at the B3LYP/6-31G(d) level over the B3LYP/6-31+G(d,p) geometries

Tautomer	α_{aa}	α_{ab}	α_{bb}	α_{cc}	$\bar{\alpha}^a$	$\Delta\alpha^b$	$\bar{\alpha}_{\text{expt.}}{}^c$
G1	121.6	−3.95	94.6	32.9	83.0	78.8	91.8
[d]	137.9	−3.4	114.6	57.5	103.3	71.9	
G2a	125.3	−3.43	92.7	32.4	83.5	81.7	
G2b	120.5	−0.68	90.6	32.3	81.1	77.6	
G3a	120.6	0.63	94.4	32.5	82.5	78.4	
G3b	118.3	3.31	96.3	32.5	82.3	77.2	
G4	110.9	1.69	99.2	33.7	81.3	72.1	
G5	120.7	−1.93	93.8	33.0	82.5	77.9	

[a] $\bar{\alpha} = (\alpha_{aa} + \alpha_{bb} + \alpha_{cc})/3$, where α_{aa}, α_{bb}, and α_{cc} are the eigenvalues of the polarizability tensor.
[b] $\Delta\alpha = \left(1/\sqrt{2}\right)[(\alpha_{aa} - \alpha_{bb})^2 + (\alpha_{aa} - \alpha_{cc})^2 + (\alpha_{bb} - \alpha_{cc})^2]^{1/2}$.
[c] The experimental datum of Ref. [26].
[d] The MP2 values of Ref. [11].

mental value of dipole moment of guanine is unknown. The magnitude of the dipole moment is strongly related to the tautomeric stability in polar environments, this distribution will be discussed in the next part (Table 5). A full table of polarizabilities of the guanine tautomers is presented as Table 3. The values of the dipole polarizabilities ($\bar{\alpha}$) and their anisotropies ($\Delta\alpha$) have no significant differences among the seven tautomers. When comparing the value of G1 in this work with the previous MP2 values [11], and the experimental value [26], we find that the present $\bar{\alpha}$ value is 10.1% lower, and the MP2 value is 12.5% higher than the experimental value. We think that the present deviation is perhaps caused by the extrapolated calculations with the smaller 6-31G(d) basis set.

3.3. Tautomeric equilibrium

Thirty-six tautomers of guanine were studied by Sabio et al. through the AM1//AM1, SCF(3-21G)//AM1, SCF(3-21G)//AM1, and SCF(3-21G)//SCF(3-21G) level calculations, their relative energies and dipole moments were tabulated, three of them (G1, G2a, and G2b as presented in Fig. 1(a) of this work) were thought to be the most stable [16]. Some theoretical studies such as MINDO/2 [12], MNDO [12], SCF/STO-3G [12], and SCF(STO-3G)//AM1 [16] suggest that G5 is more stable than G1 in vacuum. Although there is the pronounced effect of the basis set extension at the MP2, HF, and DFT(B3LYP) levels, the results showed that energy of G5 is about 0.81–1.98 kJ mol^{-1} higher than that of G1 [6]. It is very

Table 4
(Electronic energies/E_h)+538 and zero-point vibrational energies (ZPVEs/kcal mol^{-1}) of the guanine tautomers and transition states predicted at the different computational levels over the B3LYP/6-31+G(d,p) geometries

Methods	G1	G2a	G2b	G3a	G3b	G4	G5
B3LYP/6-31+G(d,p)	−4.5915	−4.5905	−4.5894	−4.5689	−4.5656	−4.5603	−4.5925
B3LYP/6-31G(d)	−4.5500	−4.5465	−4.5452	−4.5273	−4.5241	−4.5183	−4.5502
B3LYP/D95V(d)	−4.6379	−4.6350	−4.6342	−4.6145	−4.6113	−4.6065	−4.6387
XαPL/6-31G(d)	−3.2370	−3.2345	−3.2339	−3.2137	−3.2101	−3.2037	−3.2381
XαLYP/6-31G(d)	−0.8104	−0.8089	−0.8085	−0.7869	−0.7833	−0.7769	−0.8116
HF/6-31G(d)	−1.3882	−1.3865	−1.3847	−1.3649	−1.3615	−1.3557	−1.3871
ZPVE[a]	73.3321	73.2033	73.1703	72.9116	72.6173	72.7359	73.4167
Transition states[b]							
TS(1-2a)	E_h	−4.4906	ZPVE	70.1895			
TS(1-3a)		−4.4679		69.2244			
TS(1-5)		−4.4604		70.1293			

[a] The values calculated at the B3LYP/6-31G(d) level.
[b] The values calculated at the B3LYP/6-31G(d)//B3LYP/6-31G(d) level.

interesting that Gorb and Leszczynski [7], Leszczynski [21] also presented the different orders among G1, G2a, and G5, their most of the results showed that G1 is much more stable than G5 in vacuum, but the relative energy between G5 and G1 predicted at the MP2/6-31G** level calculations over the HF/6-31G** optimized geometries were surprisingly large – 129.0 kJ mol^{-1} (∼−31 kcal mol^{-1}) [21], which indicates the great freedom in the optimization would significantly change the relative energies, while both d polarization functions on the second-row elements and electron correlation effect are necessary to predict the relative energies of guanine tautomers [21]. The relative energies of the minima and transition states obtained through the single-point calculations of this work are reported in Table 4. Comparing the relative energies predicted at the B3LYP/6-31+G(d,p) and the B3LYP/6-31G(d) levels over the B3LYP/6-31+G(d,p) geometries, we find that the extrapolated calculations with the smaller basis sets may lead to the present energy deviation, ∼0.04 hartree (∼25 kcal mol^{-1}), the similar effect exists for the B3LYP/D95V(d) level calculations. It is notable that the non-local LYP functional has stronger correlation energy than the local PL functional, when we compare the relative energies calculated at the XαPL and the XαLYP levels. Our previous experiences show that there are very few differences of ZPVEs calculated at the B3LYP level using the 6-31G(d) and 6-31+G(d,p) basis sets. The different functionals and the basis sets are employed for the present calculations, but the stability order of the tautomeric forms in vacuum remains substantially unchanged (Table 5), G5 > G1 > G2a > G2b > G3a > G3b > G4, which is in agreement with our previous conclusion that the DFT methods are reliable in predicting the stability order [15]. Here G1, G2a, and G5 are three most stable tautomers, which are just as the previous conclusions and supported by the experimental IR spectrum [17–19]. Both the previous high-level calculations [6] and the present DFT results indicate that the relative energy between G1 and G5 is no more than 1 kcal mol^{-1}. The phenomenon of G2a's stability sensitive to the theoretical levels is almost not observed as Leszczynski's work [6,7], but it is true that the energy of G2a is close to those of G1 and G5. Transition states are characterized which indicate sizeable energy barrier for such processes G1 ↔ G2a, G1 ↔ G3a, G1 ↔ G5, they are ∼35, ∼45, and ∼55 kcal mol^{-1}, respectively. The barrier could be significantly decreased by interactions with a polar environment in DNA moiety, and because of the large discrepancy of the dipole moments between G1 and G5, it is apparent that the stability order of the tautomers G1 and G5 is reversed on going from the gas phase to solution, which is also proved in the calculations for solvent effect. The

SCRF calculations using the Onsager model and the PCM predict different stability orders, but they agree to stability ordering, G1 > G5 > G2a(b), in water solution. This result is in agreement with the results obtained at MP2/6-31G(d)//MP2/6-31G(d) level using the Onsager model [7], the previous experimental results also showed that both the 7-H tautomer and the 9-H tautomer of purine are predominant in vacuum and in aqueous solutions at room temperature [45]. The observation that G1 is more stable in water solution, and less stable in vacuum than G5, implies that the proton at N7 is more acidic than that at N9. This is in qualitative agreement with the conclusion that the Watson–Crick model of guanine–cytosine pair is much more stable than the Hoogsteen and the reverse-Hoogsteen models [46]. The different stability orders for other tautomers in water solution, which we believe partly, result from bad choices of the default atomic radii in the GAUSSIAN 98W program and the present calculations without the structural relaxation in solution environment. To investigate how the solute/solvent interactions affect on stability and intramolecular proton-shift, Gorb and Leszczynski [6,7], and Smedarchina et al. [47] simulated with guanine-$(water)_n$ cluster model at quantum chemical levels. It is very interesting that the stability orders of guanine(G1, G5, or G2a)-water clusters are close to the present results with the Onsager model when the number of water increases to two molecules [7]. Although the oxo (G1) and hydroxo (G2a) forms are separated by a high barrier ($\sim$35 kcal mol^{-1}), the transition can be catalyzed by water [47]. For normal spectroscopic experiments with gas samples, it is necessary to discuss tautomeric distribution with temperature.

The relative energy between G1 and G2a in vacuum obtained at the B3LYP/6-31+G(d,p) level with the ZPVE corrections, 0.52 kcal mol^{-1}, is in good agreement with the results of the simple model (where the difference between formamide and formamidic acid is used to simulate the lactam-to-lactim tautomerism of guanine) at the MP2, MP4 and couple-cluster single and double excitation (CCSD) level calculations [4]. The relative energies in vacuum predicted at the B3LYP/6-31+G(d,p)//B3LYP/6-31+G(d,p) level with the ZPVE corrections enable us to estimate the percentage of constituents of the guanine sample at the different temperatures. Assuming that only four tautomers present in the sample and adopting the equilibrium rate constant in the exponential form, G1:G2a:G2b:G5 = $1:\exp(-0.52/RT):\exp\times(-1.15/RT):\exp(0.51/RT)$, where $R = 1.99389\times 10^{-3}$ kcal mol^{-1} K^{-1} and T is the temperature. In gas phase at $T\sim 500$ K, the contribution ratio of four forms, G1:G2a:G2b:G5, equals to 10:6:3:17. The activation energies of the proton-transfer reactions can be calculated from the values obtained at the B3LYP/6-31+G(d,p)//B3LYP/6-31G(d) level in Table 5. The correction for ZPVE lowers the barriers by about 3.5 kcal mol^{-1} with respect to the values based on the electronic energies. The extended study in this work is the thermodynamic and kinetic investigation on the distribution of the tautomeric species in gas phase. The prototropic tautomerism is considered as a first-order A $\leftrightarrow$ B reaction, transition state theory [27] can be applied to calculate the rate constant k,

$$k = \Gamma\left(\frac{\kappa_B T}{h}\right)\frac{Q_{TS}}{Q_A}\exp\left(-\frac{\Delta E_0^{\neq}}{RT}\right) \quad (1)$$

and Wigner's tunneling correction [48],

$$\Gamma = 1+\frac{1}{24}\left(\frac{h\nu_{TS}}{\kappa_B T}\right)^2, \quad (2)$$

where Q_{TS} and Q_A are the partition functions of the transition state and the reactant, ν_{TS} is the imaginary frequency of the transition state. For the G1 $\leftrightarrow$ G2a, G1 $\leftrightarrow$ G3a, and G1 $\leftrightarrow$ G5, the $\log k$ vs. T profiles are plotted in the interval 300–650 K (assuming $Q_{TS}/Q_A = 1$) (Fig. 2). The profiles show that the reaction G1 $\leftrightarrow$ G2a with $\Delta E_0^{\ddagger} = 35$ kcal mol^{-1} has an appreciable rate constant at 450–650 K, and G1, G2a, G3a, and G5 would coexist at higher temperature. So the present work suggests that there would be more than three pieces of guanine tautomers presented as the IR spectra [17–19].

4. Conclusion

Geometries of the seven tautomeric species of the guanine have been presented. Most of them

Table 5
Relative energies (kcal mol^{-1}) of the guanine tautomers predicted at the different levels over the B3LYP/6-31+G(d,p) geometries

Method	G1	G2a	G2b	G3a	G3b	G4	G5
Gas phase							
B3LYP/6-31+G(d,p)	0.0	0.65	1.31	14.19	16.25	19.57	−0.59
B3LYP/6-31+G(d,p)+ZPVE[a]	0.0	0.52	1.15	13.78	15.53	18.99	−0.51
XαLYP/6-31G(d)	0.0	0.97	1.22	14.75	17.02	21.03	−0.76
XαPL/6-31G(d)	0.0	1.59	1.93	14.66	16.89	20.89	−0.69
B3LYP/6-31G(d)	0.0	2.20	3.01	14.24	16.25	19.89	−0.13
B3LYP/D95V(d)	0.0	1.83	2.30	14.66	16.88	19.72	−0.51
HF/6-31G(d)	0.0	1.09	2.24	14.65	16.75	20.42	−0.70
B3LYP/6-311++G(df,pd)[b]	0.0	2.10					−0.38
	0.0	1.08					−0.43
MP2/6-311++G(df,pd)[b]	0.0	−0.87					−0.27
	0.0	−1.02					−0.19
Solvent effects[c]							
Onsager model	0.0	7.58	7.57	15.80	9.44	4.38	7.63
PCM	0.0	5.12	6.64	11.69	11.68	10.52	0.72

[a] ZPVEs calculated at the B3LYP/6-31G(d) level and scaled with the factor 0.9804.
[b] Single-point energies calculated over the B3LYP/6-311++G(df,dp) geometries [6,7] in the first line or the MP2/6-31G(d,p) geometries in the second line.
[c] The B3LYP/6-31+G(d,p) values of the tautomers in water ($\varepsilon = 78.39$) solution without the structural relaxation.

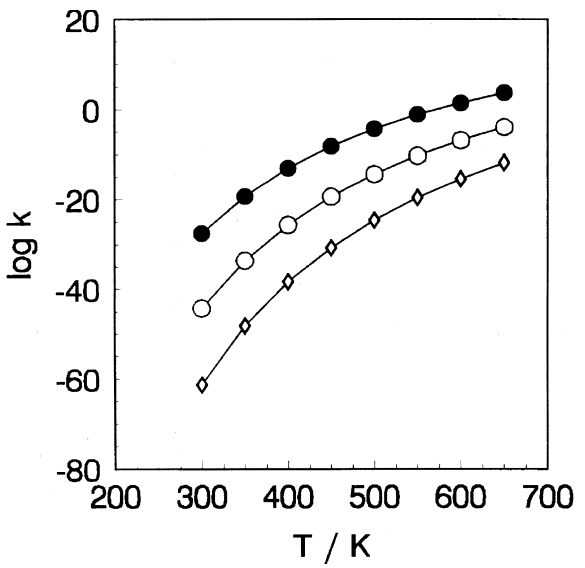

Fig. 2. Log$k$ vs. T profiles calculated using Eqs. (1) and (2): (●), the G1 ↔ G2a reaction with $\Delta E_0^{\ddagger} = 35$ kcal mol^{-1}, $\nu_{TS} = 1990$ cm^{-1}; (○), the G1 ↔ G3a reaction with $\Delta E_0^{\ddagger} = 45$ kcal mol^{-1}, $\nu_{TS} = 1990$ cm^{-1}; (◇), the G1 ↔ G5 reaction with $\Delta E_0^{\ddagger} = 55$ kcal mol^{-1}, $\nu_{TS} = 1550$ cm^{-1}.

have coplanar purine rings. The dipole moments, dipole polarizabilities and their components and anisotropies are obtained and compared with the previously theoretical data and experimental result. The present DFT calculations predicted that the stability order of the tautomers in vacuum is G5 > G1 > G2a > G2b > G3a > G3b > G4, while some are reversed in water solution because of the significant differences of the magnitude of dipole moments in vacuum. The difficulties encountered in the identification of spectroscopy experiments are due to the kinetic effects, because the G1 ↔ G2a, G1 ↔ G3a, and G1 ↔ G5 reactions have the appreciable rate constant at $T \sim 650$ K. However, there are still some experimental methods for identifying the tautomeric species, for examples, according to solution effects, the ^{13}C and ^{15}N NMR measurements can distinguish G1 and G5 species in aqueous solutions [49]. As the large energy barrier of G1 ↔ G5 reaction in vacuum, if one of them would be purified using some chemical technique, the single kind of tautomers could be studied through spectroscopic measurements at low temperature [50].

Acknowledgements

This work was supported in part by the National Natural Science Foundation of China. The

author S.X.T. is a JSPS post-doctoral research fellow (2000–2002).

References

[1] M.D. Topal, J.R. Fresco, Nature 263 (1986) 285.
[2] M.D. Topal, J.R. Fresco, Nature 263 (1986) 289.
[3] M.J. Scalan, I.H. Hillier, J. Am. Chem. Soc. 106 (1984) 3737.
[4] J.S. Kwiatkowski, R.J. Bartlett, W.B. Person, J. Am. Chem. Soc. 110 (1988) 2353.
[5] C. Roberts, R. Bandaru, C. Switzer, J. Am. Chem. Soc. 119 (1997) 4640, and references therein.
[6] J. Leszczynski, J. Phys. Chem. A 102 (1998) 2357.
[7] L. Gorb, J. Leszczynski, J. Am. Chem. Soc. 120 (1998) 5024.
[8] P.G. Jasien, G. Fitzgerald, J. Chem. Phys. 93 (1990) 2554.
[9] E.L. Stewart, C.K. Foley, N.L. Allinger, J.P. Bowen, J. Am. Chem. Soc. 116 (1994) 7283.
[10] J. Sponer, P. Hobza, J. Phys. Chem. 98 (1994) 3161.
[11] R.C. Johnson, T.D. Power, J.S. Holt, B. Immaraporn, J.E. Monat, A.A. Sissoko, M.M. Yanik, A.V. Zagoradny, S.M. Cybulski, J. Phys. Chem. 100 (1996) 18875, and references therein.
[12] T.J. Zielinski, D.L. Breen, K. Haydok, R. Rein, R.D. MacElory, Int. J. Quant. Chem. (1978) 355.
[13] W.B. Person, K. Szczepaniak, M. Szczepaniak, J.S. Kwiatkoeski, L. Hernandaz, R. Czerminski, J. Mol. Struct. 194 (1989) 239.
[14] S. Morpurgo, M. Bossa, G.O. Morpurgo, Chem. Phys. Lett. 280 (1997) 233.
[15] S.X. Tian, C.F. Zhang, Z.J. Zhang, X.J. Chen, K.Z. Xu, Chem. Phys. 242 (1999) 217, and references therein.
[16] M. Sabio, S. Topiol, W.C. Lumma Jr., J. Phys. Chem. 94 (1990) 1366.
[17] K. Szczepaniak, M. Szczepaniak, W. Szajda, W.B. Person, J. Leszczynski, J. Can. Chem. 69 (1991) 1718.
[18] M. Graindourze, Y. Smets, Th. Zeegers-Huyskens, G. Maes, J. Mol. Struct. 222 (1990) 345.
[19] K. Szczepaniak, M. Szczepaniak, J. Mol. Struct. 151 (1987) 294.
[20] I.R. Gould, I.H. Hillier, Chem. Phys. Lett. 161 (1989) 185.
[21] J. Leszczynski, Chem. Phys. Lett. 174 (1990) 347.
[22] I.R. Gould, N.H. Burton, R.J. Hall, I.H. Hillier, J. Mol. Struct. (Theochem) 331 (1995) 147.
[23] C. Roberts, R. Bandarn, C. Switzer, J. Am. Chem. Soc. 119 (1997) 4640.
[24] J. Lin, C. Yu, S. Peng, I. Aklyama, K. Li, L.K. Lee, P.R. LeBreton, J. Phys. Chem. 84 (1980) 1006.
[25] P.R. LeBreton, X. Yang, S. Urano, S. Fetzer, M. Yu, N.J. Leonard, S. Kumar, J. Am. Chem. Soc. 112 (1990) 2138.
[26] C.F.J. Bottcher, Theory of Electric Polarization, Elsevier, Amsterdam, 1952.
[27] P.W. Atkins, Physical Chemistry, 2nd ed., Oxford University Press, Oxford, 1982.
[28] M.J. Frisch, G.W. Trucks, H.B. Schlegel, G.E. Scuseria, M.A. Robb, J.R. Cheeseman, V.G. Zakrzewski, J.A. Montgomery Jr., R.E. Stratmann, J.C. Burant, S. Dapprich, J.M. Millam, A.D. Daniels, K.N. Kudin, M.C. Strain, O. Farkas, J. Tomasi, V. Barone, M. Cossi, R. Cammi, B. Mennucci, C. Pomelli, C. Adamo, S. Clifford, J. Ochterski, G.A. Petersson, P.Y. Ayala, Q. Cui, K. Morokuma, D.K. Malick, A.D. Rabuck, K. Raghavachari, J.B. Foresman, J. Cioslowski, J.V. Ortiz, A.G. Baboul, B.B. Stefanov, G. Liu, A. Liashenko, P. Piskorz, I. Komaromi, R. Gomperts, R.L. Martin, D.J. Fox, T. Keith, M.A. Al-Laham, C.Y. Peng, A. Nanayakkara, C. Gonzalez, M. Challacombe, P.M.W. Gill, B. Johnson, W. Chen, M.W. Wong, J.L. Andres, C. Gonzalez, M. Head-Gordon, E.S. Replogle, and J.A. Pople, GAUSSIAN 98, Revision A.7, Gaussian, Inc., Pittsburgh PA, 1998.
[29] B.G. Johnson, P.M.W. Gill, J.A. Pople, J. Chem. Phys. 98 (1993) 5612.
[30] P.J. Stephens, F.J. Devlin, C.F. Chabalowski, M.J. Frisch, J. Phys. Chem. 98 (1994) 11623.
[31] F.J. Deviln, J.W. Finley, P.J. Stephens, M.J. Frisch, J. Phys. Chem. 98 (1995) 16883.
[32] A.D. Becke, J. Chem. Phys. 98 (1993) 1372.
[33] A.D. Becke, J. Chem. Phys. 98 (1993) 5648.
[34] C. Lee, W. Yang, R.G. Parr, Phys. Rev. B 27 (1988) 785.
[35] T.H. Dunning Jr., P.J. Hay, Modern Theoretical Chemistry, in: H.F. Schaefer III (Ed.), Plenum Press, New York, 1976, vol. 3, p. 1.
[36] J.C. Slater, Quantum Theory of Molecular and Solids, vol. 4: The Self-Consistent Field for Molecular and Solids, McGraw-Hill, New York, 1974.
[37] J.P. Perdew, A. Zunger, Phys. Rev. B 33 (1981) 5048.
[38] M.W. Wong, Chem. Phys. Lett. 256 (1996) 391.
[39] Æ. Frisch, M.J. Frisch, GAUSSIAN 98 User's Reference, Gaussian, Inc., Pittsburgh, USA, 1998, and references therein.
[40] L.J. Onsager, J. Am. Chem. Soc. 58 (1936) 1486.
[41] M.M. Karelson, M.C. Zerner, Int. J. Quant. Chem. Symp. 20 (1986) 521.
[42] M.M. Karelson, M.C. Zerner, J. Phys. Chem. 96 (1992) 8991.
[43] M.W. Wong, K.B. Wiberg, M.J. Frisch, J. Am. Chem. Soc. 114 (1992) 1645.
[44] S. Miertus, E. Scrocco, J. Tomasi, Chem. Phys. 55 (1981) 117.
[45] A. Broo, A. Holmen, Chem. Phys. 211 (1996) 147, and references therein.
[46] B. Pullman et al., in: J.N. Davidson (Ed.), Progress in Nucleic Acid Research and Molecular Biology, Academic Press, New York, London, 1969.
[47] Z. Smedarchina, W. Siebrand, A. Fernanadez-Ramos, L. Gorb, J. Leszczynski, J. Chem. Phys. 112 (2000) 566.

[48] E. Wigner, Z. Phys. Chem. 19 (1932) 203.
[49] N.C. Gonnella, J.D. Roberts, J. Am. Chem. Soc. 104 (1982) 3162, and references therein.
[50] M.J. Nowak, H. Rostkowska, L. Lapinski, J.S. Kwiatkowski, J. Lezczynski, J. Phys. Chem. 98 (1994) 813, and references therein.